

Supporting information

Enhanced high-temperature energy storage properties of polymer composites by interlayered metal nanodots

Shuai Li^{a#}, Jiufeng Dong^{a,b#}, Yujuan Niu^a, Li Li^a, Feng Wang^a, Renchao Hu^a, Jin Cheng^a, Liang Sun^a, Zizhao Pan^a, Xinwei Xu^a and Hong Wang^{a*}

^a Department of Materials Science and Engineering, Southern University of Science and Technology, Shenzhen 518055, China.

Shenzhen Engineering Research Center for Novel Electronic Information Materials and Devices, Southern University of Science and Technology, Shenzhen 518055, China.

Guangdong Provincial Key Laboratory of Functional Oxide Materials and Devices, Southern University of Science and Technology, Shenzhen 518055, China.

^b School of Microelectronics, State Key Laboratory for Mechanical Behavior of Materials, Xi'an Jiaotong University, Xi'an 710049, China.

E-mail: wangh6@sustech.edu.cn

These authors contribute equally to this work.

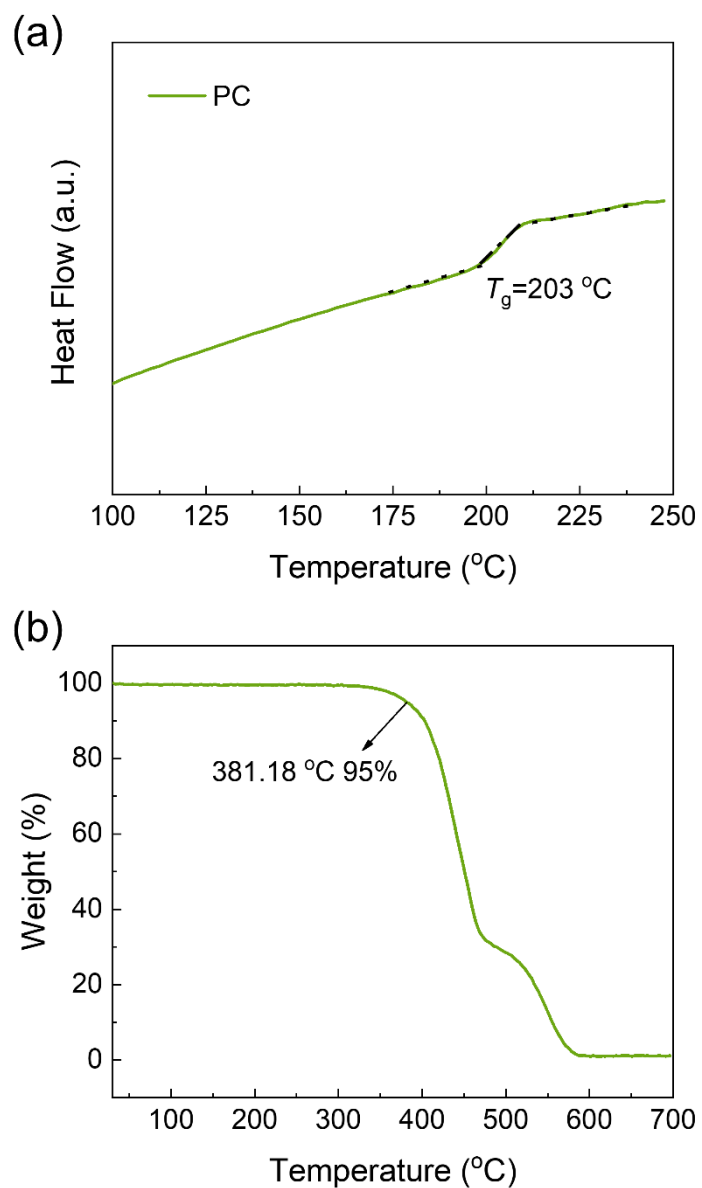


Fig. S1. (a) DSC curves of polycarbonate (PC) film. (b) TGA curve of pristine PC film.

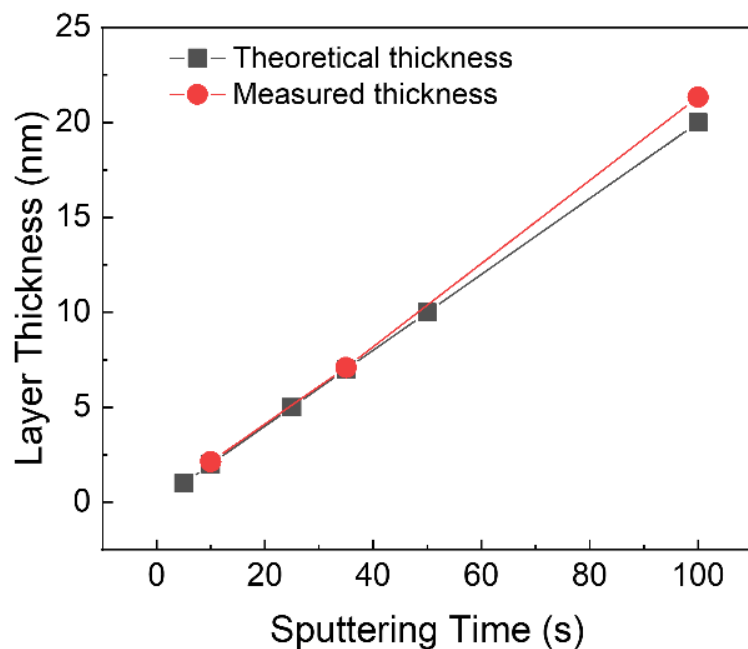


Fig. S2. Layer thickness as a function of time for the sputtered Au layer.

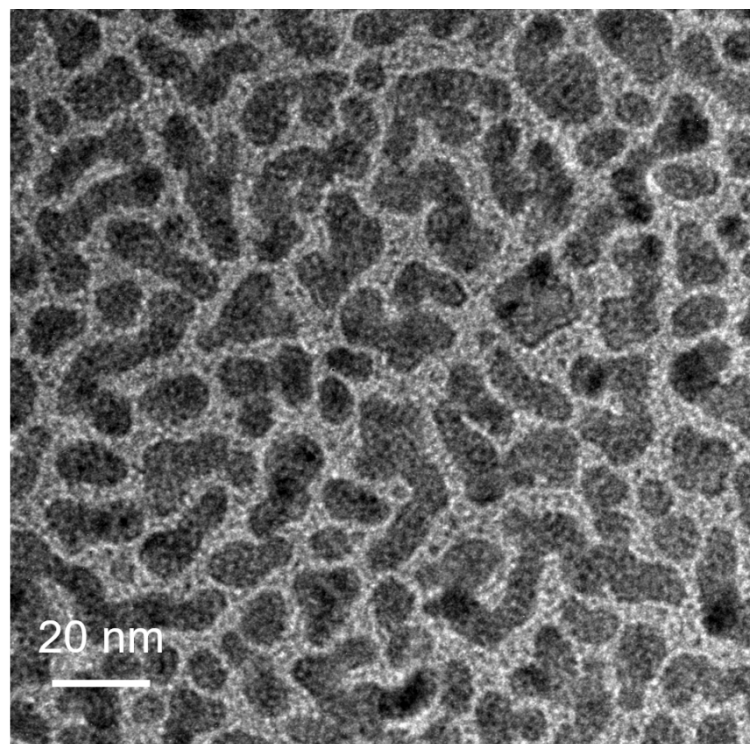


Fig. S3. TEM bright field images of the sputtered 35 s Au.

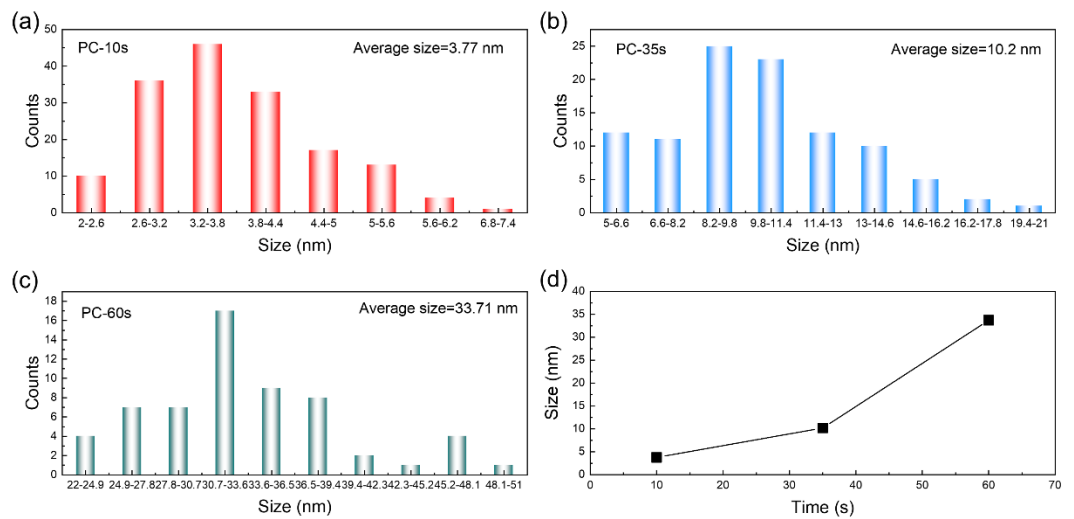


Fig. S4. Size of the diameter statistical histograms of (a) Au-10s, (b) Au-35s, and (c) Au-60s. (d) The dependence of the size of Au nanodots with sputtering time.

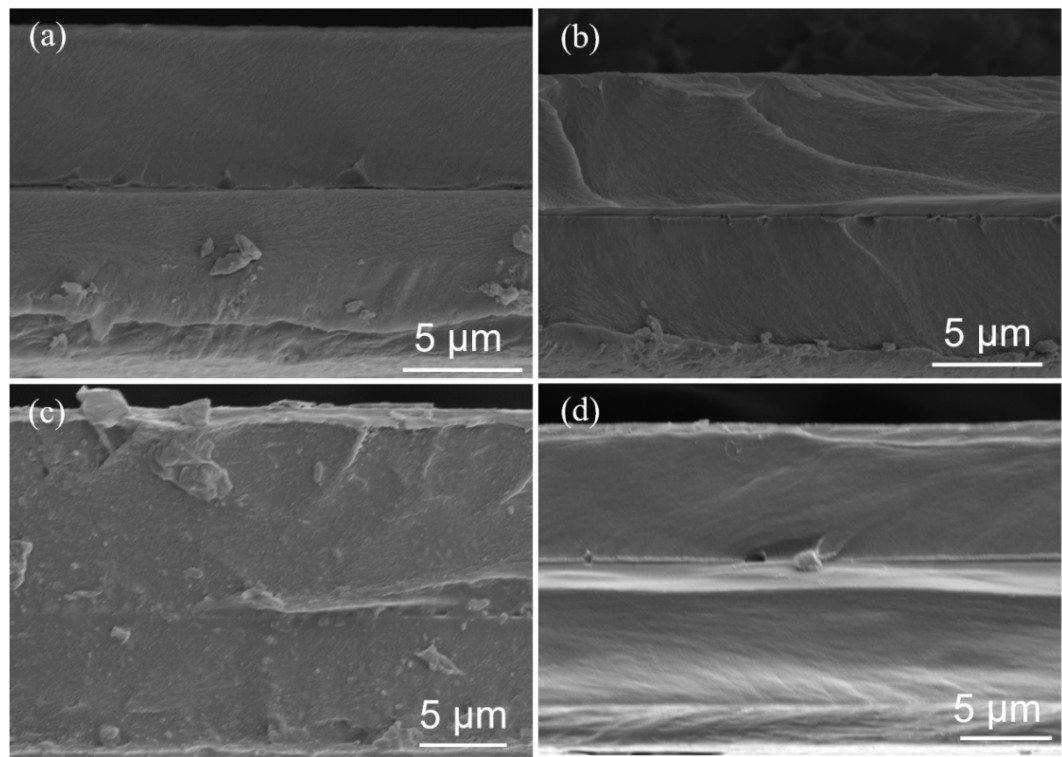


Fig. S5. Cross-section scanning electron microscope (SEM) images of metal-polymer composite materials for (a) PC-5s, (b) PC-10s, (c) PC-25s, (d) PC-35s.

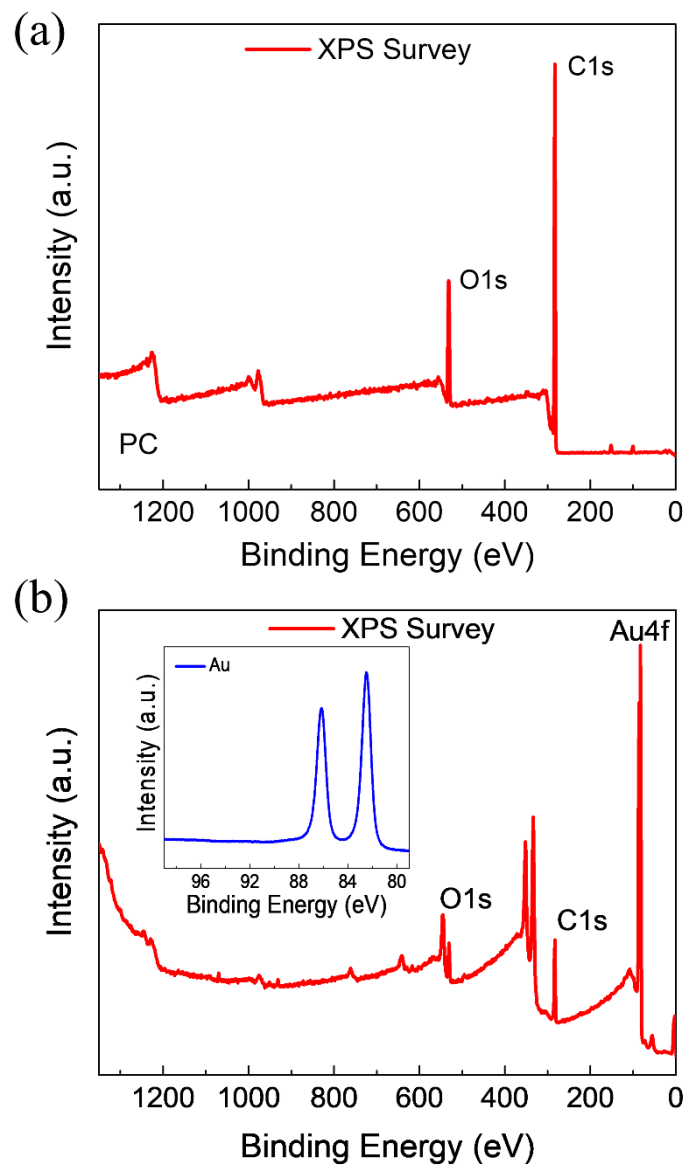


Fig. S6. X-ray photoelectron spectroscopy (XPS) survey of the (a) pure PC and (b) PC-10s films. The inset in (b) is the core-level XPS spectra of $\text{Au}4\text{f}$.

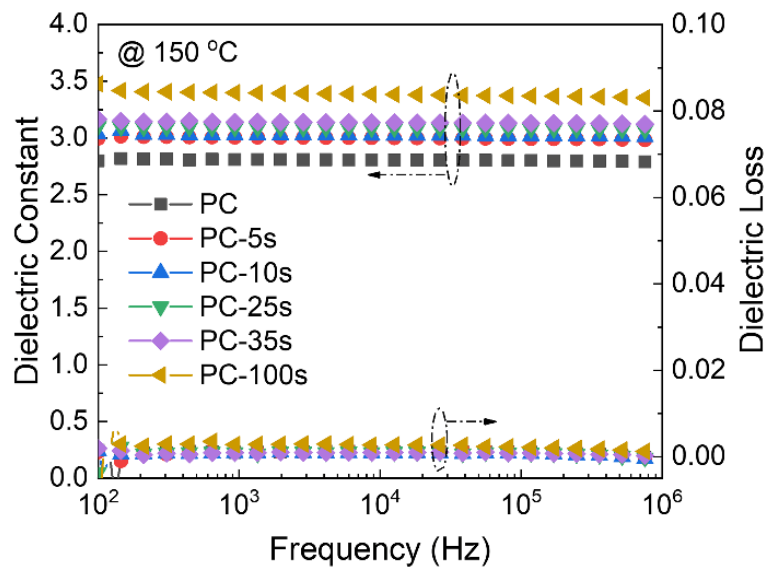


Fig. S7. Frequency-dependent dielectric spectra of the films with varied frequencies ranging from 100 Hz to 1 MHz at 150 °C.

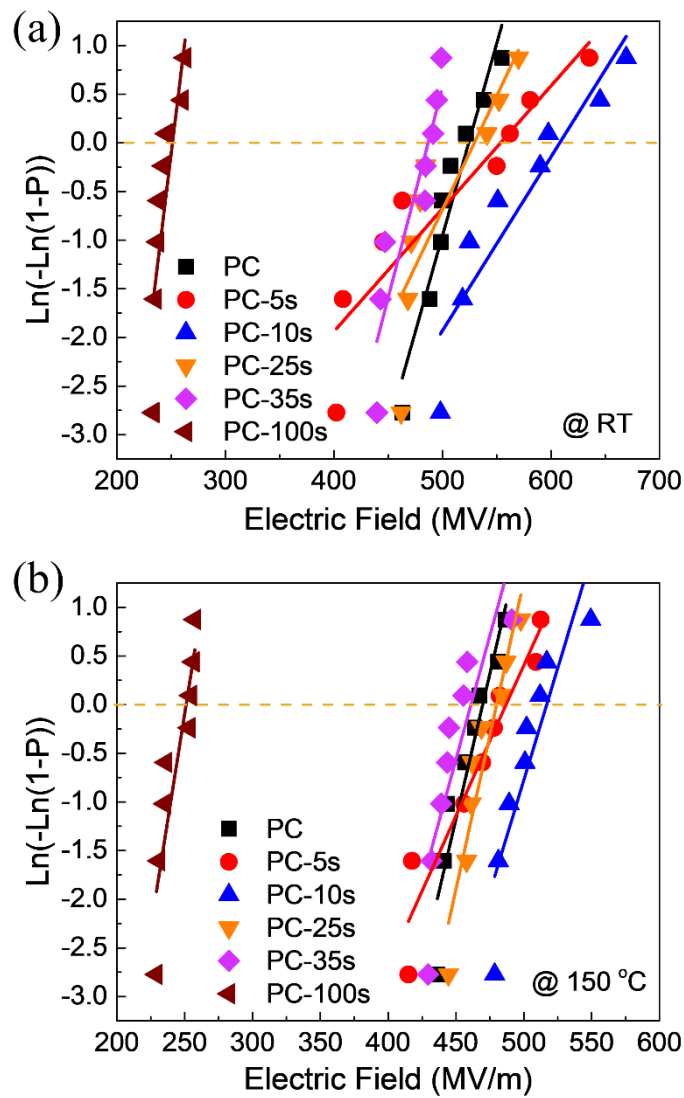


Fig. S8. Weibull statistic of dielectric breakdown strength of PC-based interlayer metal-polymer composites at (a) room temperature and (b) 150 °C.

Table S1. Weibull parameters of heterojunction films with different sputter time at varying temperatures.

Temperature	Parameter	PC	PC-5s	PC-10s	PC-25s	PC-35s	PC-100s
Room temperature	E_b (MV m ⁻¹)	523	555	609	530	487	282
	β	20.71	6.99	10.86	12.36	21.03	22.91
150 °C	E_b (MV m ⁻¹)	470	487	518	480	462	251
	β	28.05	15.06	23.79	30.38	23.48	22.04

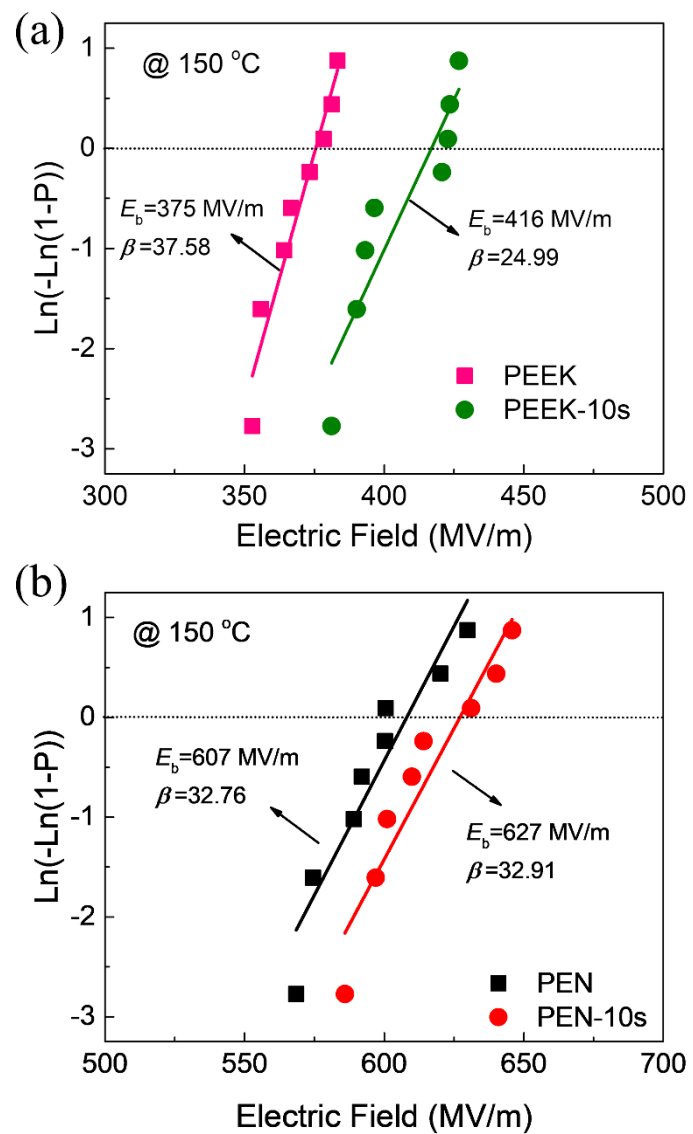


Fig. S9. Weibull statistic of dielectric breakdown strength of (a) PEEK-based interlayer metal-polymer composites at 150 °C and (b) PEN-based interlayer metal-polymer composites at 150 °C.

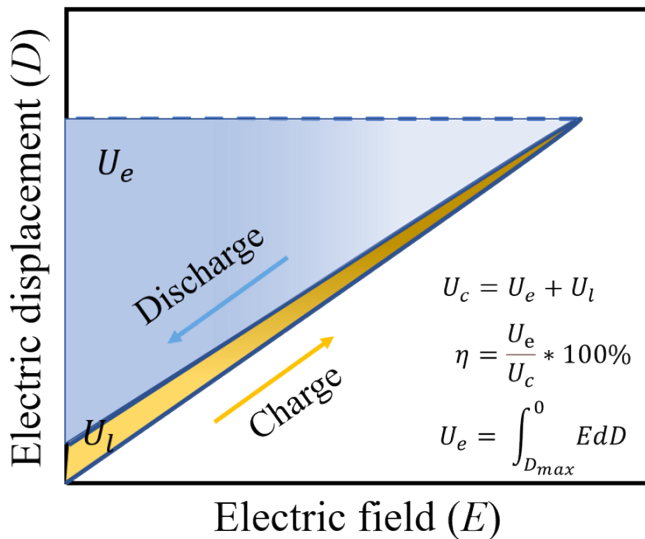


Fig. S10. Schematic polarization-electric field (P - E) loop of dielectric materials, where the charged energy density (U_c) is derived from the P - E loop by integration of the area between the charge curve and ordinate, the discharged energy density (U_e) is determined by the area between the discharge curve and the ordinate, and the efficiency (η) is the ratio of U_e and U_c .

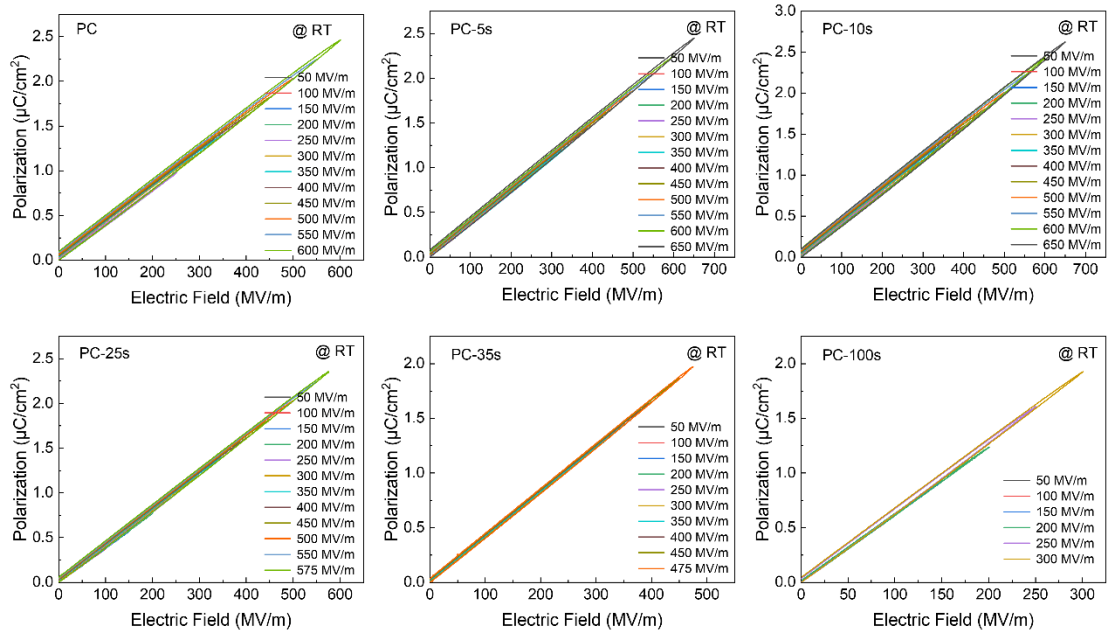


Fig. S11. P - E loops of PC-based layer-structured metal–polymer composites at room temperature and different electric fields.

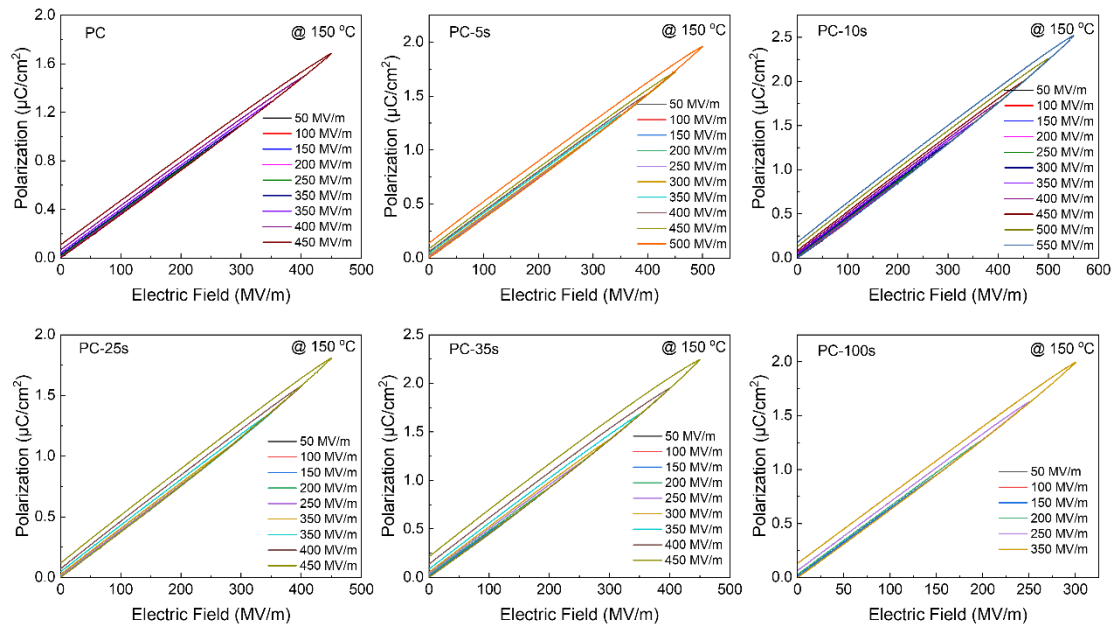


Fig. S12. P - E loops of PC-based layer-structured metal–polymer composites at 150 °C and different electric fields.

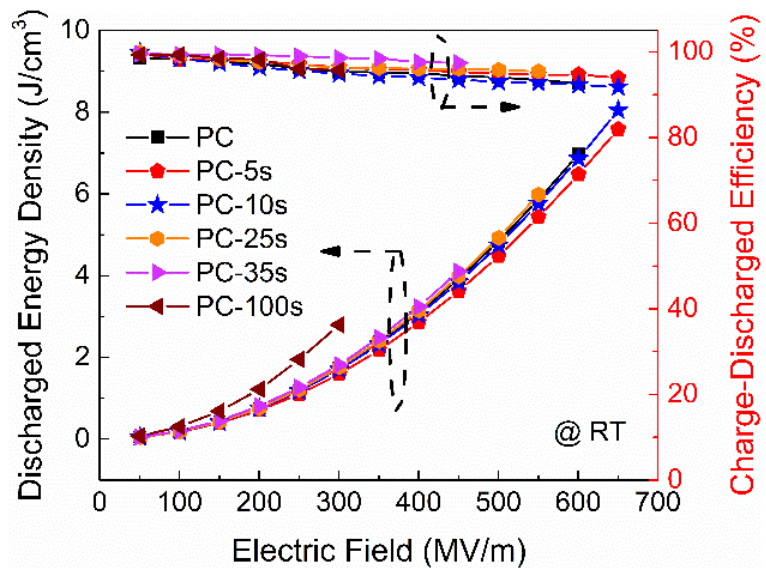


Fig. S13. Energy storage performance of PC-based interlayer metal-polymer composites at room temperature.

Table S2. The dielectric properties, breakdown properties, leakage current characteristics and energy storage performance of all samples

Samples	$\epsilon_r / \tan \delta$ (10^{-3})	$J (\times 10^9 \text{ A cm}^{-2})$ @ 150 °C	$E_b (\text{MV m}^{-1})$ @ RT	$E_b (\text{MV m}^{-1})$ @ 150 °C	$U_e (\text{J cm}^{-3})$ @ RT	$\eta (\%)$ @ RT	$U_e (\text{J cm}^{-3})$ @ 150 °C	$\eta (\%)$ @ 150 °C
PC	2.86/1.1	13.6	523	470	6.97	92.6	3.47	89.3
PC-5s	3.04/1.6	4.28	555	487	7.59	93.9	4.44	87.8
PC-10s	3.14/2.8	3.86	609	518	8.05	91.8	6.25	86.6
PC-25s	3.20/4.2	6.14	530	480	5.98	95.4	4.54	85.6
PC-35s	3.24/5.3	4.02	487	462	4.10	97.4	4.38	83.5
PC-100s	3.49	1.71	282	251	2.80	95.7	2.75	89.3

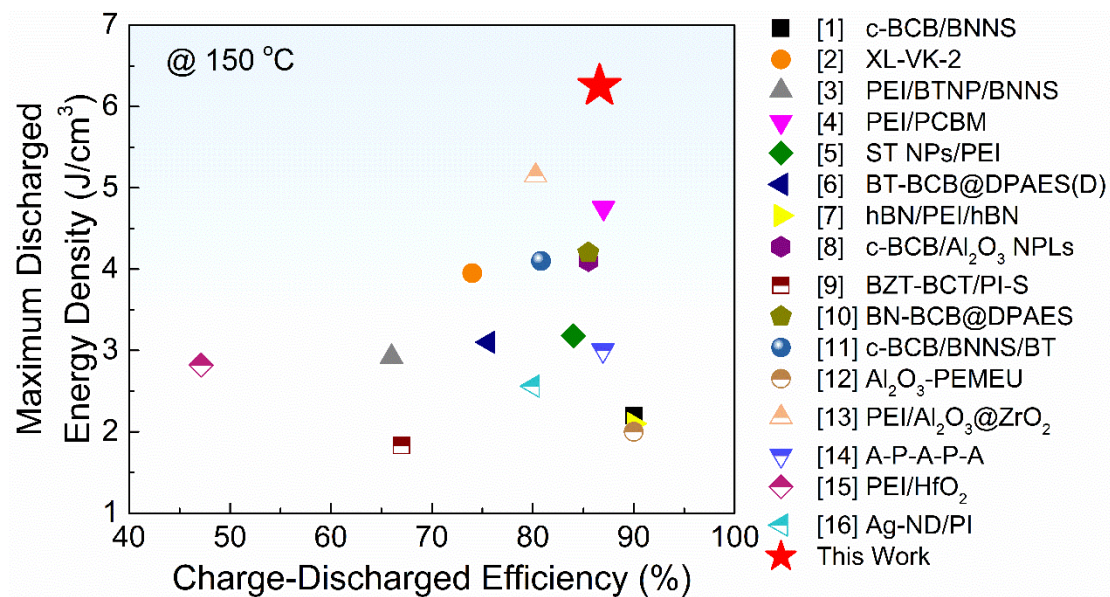


Fig. S14. Comparison of the maximum discharged energy density as a function of charge-discharged efficiency for representative dielectric materials at 150 °C[1-16].

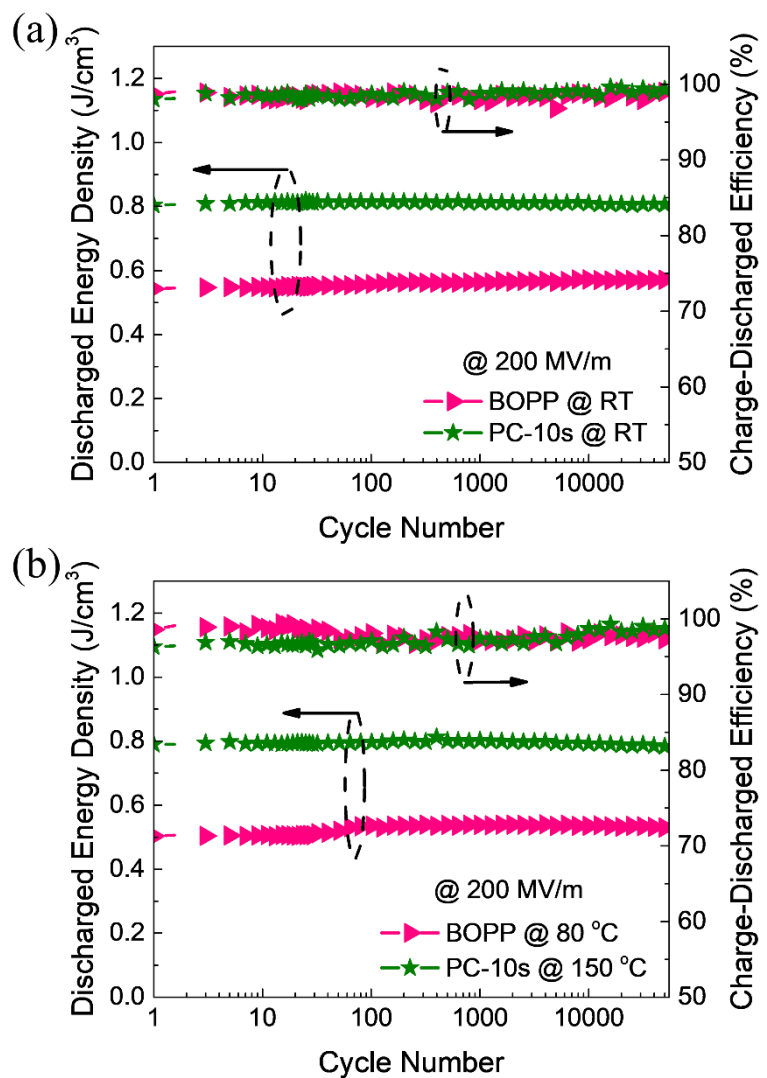


Fig. S15. Charge-discharge cycle performance of the BOPP and PC-10s under 200 MV m^{-1} at (a) room temperature and (b) elevated temperature.

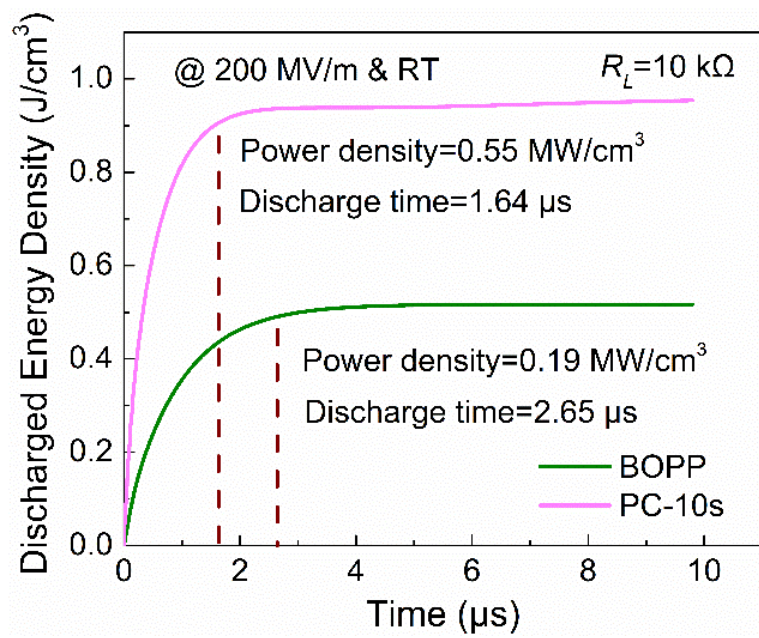


Fig. S16. Discharged energy density as a function of time for BOPP and PC-10s under 200 MV m^{-1} and room temperature.

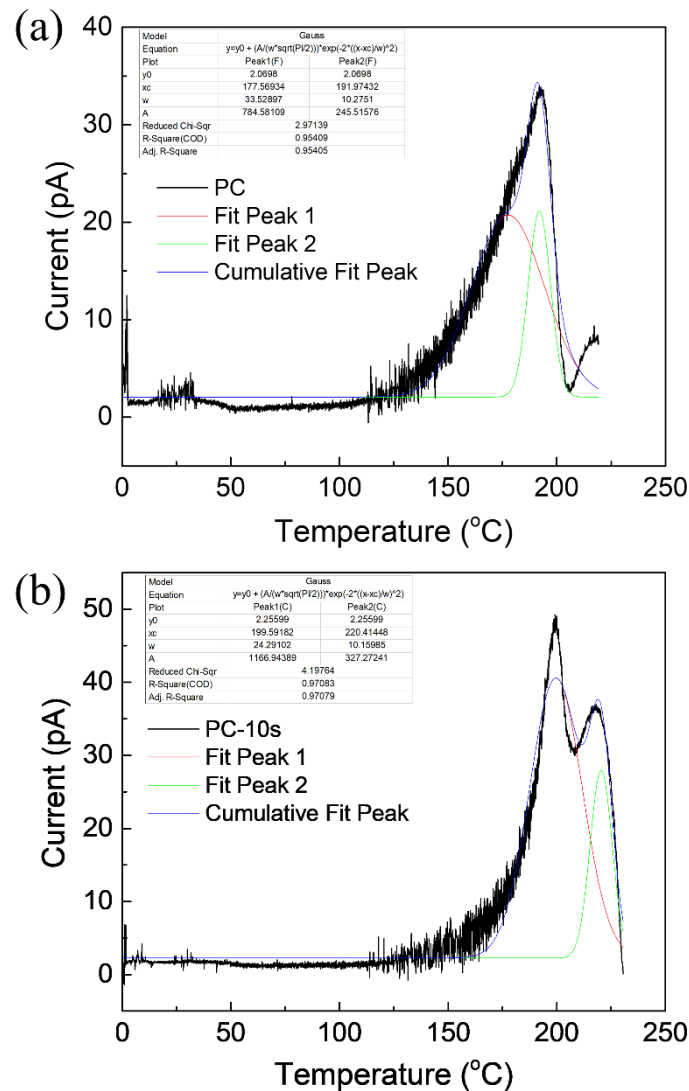


Fig. S17. TSDC and its gauss fitting curves of (a) PC and (b) PC-10s.

Table S3. TSDC results and calculated trap parameters of PC and PC-10s.

Samples	α Peak1 ($\alpha 1$)			α Peak2 ($\alpha 2$)		
	Trap Energy (eV)	Q_d (nC)	T_{m1} ($^{\circ}\text{C}$)	Trap Energy (eV)	Q_s (nC)	T_{m2} ($^{\circ}\text{C}$)
PC	0.20	15.69	177.57	0.76	4.91	191.97
PC-10s	0.35	23.34	199.59	1.02	6.55	220.41

References

- 1 Q. Li, L. Chen, M.R. Gadinski, S. Zhang, G. Zhang, U. Li, E. Iagodkine, A. Haque, L.Q. Chen, N. Jackson and Q. Wang, *Nature*, 2015, **523**, 576-579.
- 2 H. Li, M.R. Gadinski, Y. Huang, L. Ren, Y. Zhou, D. Ai, Z. Han, B. Yao and Q. Wang, *Energy Environ. Sci.*, 2020, **13**, 1279-1286.
- 3 H. Li, L. Ren, D. Ai, Z. Han, Y. Liu, B. Yao and Q. Wang, *InfoMat*, 2019, **2**, 389-400.
- 4 C. Yuan, Y. Zhou, Y. Zhu, J. Liang, S. Wang, S. Peng, Y. Li, S. Cheng, M. Yang, J. Hu, B. Zhang, R. Zeng, J. He and Q. Li, *Nat. Commun.*, 2020, **11**, 3919.
- 5 W. Miao, H. Chen, Z. Pan, X. Pei, L. Li, P. Li, J. Liu, J. Zhai and H. Pan, *Compos. Sci. Technol.*, 2021, **201**, 108501.
- 6 J. Liu, Z. Shen, W. Xu, Y. Zhang, X. Qian, Z. Jiang and Y. Zhang, *Small*, 2020, **16**, 2000714.
- 7 A. Azizi, M.R. Gadinski, Q. Li, M.A. AlSaud, J. Wang, Y. Wang, B. Wang, F. Liu, L.Q. Chen, N. Alem and Q. Wang, *Adv. Mater.*, 2017, **29**, 1701864.
- 8 H. Li, D. Ai, L. Ren, B. Yao, Z. Han, Z. Shen, J. Wang, L.Q. Chen and Q. Wang, *Adv. Mater.*, 2019, **31**, 1900875.
- 9 Q. Chi, Z. Gao, T. Zhang, C. Zhang, Y. Zhang, Q. Chen, X. Wang and Q. Lei, *ACS Sustain. Chem. Eng.*, 2018, **7**, 748-757.
- 10 W. Xu, J. Liu, T. Chen, X. Jiang, X. Qian, Y. Zhang, Z. Jiang and Y. Zhang, *Small*, 2019, **15**, 1901582.
- 11 Q. Li, F. Liu, T. Yang, M.R. Gadinski, G. Zhang, L.Q. Chen and Q. Wang, *Proc. Natl. Acad. Sci. USA*, 2016, **113**, 9995-10000.
- 12 T. Zhang, X. Chen, Q. Zhang and Q.M. Zhang, *Appl. Phys. Lett.*, 2020, **117**, 072905.
- 13 L. Ren, H. Li, Z. Xie, D. Ai, Y. Zhou, Y. Liu, S. Zhang, L. Yang, X. Zhao, Z. Peng, R. Liao and Q. Wang, *Adv. Energy Mater.*, 2021, **11**, 2101297.
- 14 J. Dong, R. Hu, X. Xu, J. Chen, Y. Niu, F. Wang, J. Hao, K. Wu, Q. Wang and H. Wang, *Adv. Funct. Mater.*, 2021, **31**, 2102644.
- 15 L. Ren, L. Yang, S. Zhang, H. Li, Y. Zhou, D. Ai, Z. Xie, X. Zhao, Z. Peng, R. Liao and Q. Wang, *Compos. Sci. Technol.*, 2021, **201**, 108528.
- 16 S. Xing, Z. Pan, X. Wu, H. Chen, X. Lv, P. Li, J. Liu and J. Zhai, *J. Mater. Chem. C*, 2020, **8**, 12607-12614.